COMMUNICATIONS IN SCIENCE AND TECHNOLOGY
Homepage: cst.kipmi.or.id

A novel approach in the synthesis of CdS/titania nanotubes array nanocomposites to obtain better photocatalyst performance

Reno Pratiwi[a], M. Ibadurrohman[a], Eniya L. Dewi[b], Slamet[a,*]

[a]*Department of Chemical Engineering, Faculty of Engineering, Universitas Indonesia, Depok 16424 Indonesia*
[b]*Agency for the Assesment and Application Technology, Puspiptek, Serpong 15314, Indonesia*

Article history:
Received: 30 November 2022 / Received in revised form: 9 February 2023 / Accepted: 16 February 2023

Abstract

Studies that seek to improve the performance of photocatalyst continue to develop. Several observations have been made on the effect of using ultrasonic waves during the synthesis process of CdS/Titania Nanotubes Array (CdS/TiNTA) nanocomposites on an ability to degrade ciprofloxacin solution (CIP) and produce hydrogen. Therefore, the nanocomposite synthesis process uses the Successive Ionic Layer Adsorption and Reaction (SILAR) method, with $(CH_3COO)_2Cd$ and Na_2S as the precursors. During the SILAR process, sonication was applied for 60 minutes and carried out in the amorphous phase of TiO_2 to increase the effectiveness of contact between the two semiconductors. The synthesis results were confirmed in term of their crystallinity, morphology, the presence of components on the surface, and the shift of bandgap by means of XRD, FESEM, FTIR, and UV-Vis DRS characterization, respectively. Photocatalytic activities of the nanocomposites were evaluated in a system containing 10 ppm CIP solution, on the purpose of observing their ability to degrade CIP and produce hydrogen. Our findings revealed an improvement in crystallinity, successful semiconductor coupling, and a band gap narrowing in the synthesized nanocomposites. Furthermore, the photocatalysts synthesized in the amorphous TiO_2 and by sonication during SILAR offered doubled production capacity of hydrogen (0.191 mmol/m^2) as compared to photocatalysts synthesized without sonication (0.092 mmol/m^2). Compared to similar photocatalysts synthesized using the SILAR method in the crystalline phase, photocatalysts synthesized in the amorphous phase exhibited four-fold higher hydrogen production (0.044 to 0.191 mmol/m^2). This prominent ability of the nanocomposites is related to the success of CdS adhering well to TiO_2 surface to form nanocomposites, so that the bandgap energy position of CdS that is strong in the reduction reaction greatly contributes to improve the performance of the resulting photocatalyst, which is very advantageous in terms of its ability in water-splitting reactions.

Keywords: SILAR, sonication; CdS/TiNTA; photocatalysis

1. Introduction

Photocatalysis has been developed and progressively evolved since its discovery by Honda and Fujishima in 1972 [1]. The nature of photocatalysis is efficient cost-effective, environmentally friendly, and efficient in terms of oxidation-reduction reactions, making it attractive to researchers towards continuous development and advancement. However, the main issues that need to be resolved in this process are the lack of ability to absorb photon energy in the visible-light spectrum and the occurrence of recombination of photogenerated electron-hole pairs, dissipating their chemical energy as heat. A number of strategies used to overcome these issues include modifying the morphology of the photocatalyst surface by introducing dopants to reduce energy bandgap, and increasing an ability to absorb light using cocatalysts or sensitizers [2-6].

TiO_2 is widely used as a semiconducting photocatalyst due to its abundance,excelent stability, resistive to corrosion, and cost effectiveness [2,4,6,7]. One-dimensional TiO_2 nanotubes arrays (TiNTA) can provide convenient pathways for the transport of photogenerated electrons due to their highly ordered structure, hence suppressing the recombination of photogenerated electrons/holes and facilitating light harvesting process. However, the broad bandgap of TiNTA (3.2 eV for the anatase phase), which are only capable of absorbing ultraviolet light, still becomes an obstacle that needs to be resolved. Meanwhile, CdS with an energy bandgap value of 2.3 eV, can absorb visible light. The relative band structure of CdS and TiNTA provides a technological advantage if they can be coupled as nanocomposites that establish a heterojunction scheme, expanding the interval of usable light spectrum. Concurrently, the rate of recombination of electrons and holes can be suppressed. Many attempts have been made to form CdS/TiO_2 pairs in nanocomposite forms. SILAR is a synthesis method widely used to obtain CdS/TiO_2 nanocomposite [8-10]. Previous studies related to the development of the SILAR process, so far, were limited to determine the number of cycles and dipping time[9,11-13]. Other treatments, such as sonication are sometimes applied during the synthesis process, but they are only to clean the TiNTAs plate from post-anodization impurities [13-15]

The study on the effect of sonication's on photocatalyst

* Corresponding author.
Email: Slamet@che.ui.ac.id
https://doi.org/10.21924/cst.8.1.2023.1049

synthesis is intriguing because ultrasonic waves are believed to provide a cavitation effect, thereby increasing the effectiveness of photocatalyst synthesis products. Some of the advantages of using ultrasonic waves include the increase of the reaction speed, homogenization, dispersion, decay of molecules during the synthesis process, wider catalyst surface due to the cleaning effect occurred in sonication, the increase of the gas flow in the liquid to give a stimulating effect, and rise in pressure and temperature, which can increase the number of crystals formed [16-18].

Studies on using ultrasonic waves in synthesizing TiO_2 photocatalyst particles using several types of dopants have been carried out separately. The results showed that the improved crystallinity, surface area, and ability to absorb light exposure were the main reasons for the increased performance [16, 17, and 19]. These studies used the TiO_2 semiconductor as a titania film layer with nanotube array morphology (TiNTA). The photocatalyst performance was then improved by attaching CdS as a semiconductor coupling with the SILAR method on the amorphous phase of TiO_2. The synthesis process carried out in the amorphous hydroxylated TiO_2 phase would improve the quality of the photocatalyst [17]. In previous studies, SILAR was usually carried out on TiNTA in the crystalline phase, which failed to produce a strong bond between CdS and TiNTA [15]. Moreover, this condition resulteds in poor interfacial contact and so fast electron transfer from CdS to TiNTA, thereby increasing the recombination rate [13].

It is believed that the porous surface of the amorphous TiO_2 phase will improve the contact between TiO_2 and CdS so that a heterojunction mechanism may establish. In turn, this preferable interaction shall improve the performance of the photocatalyst (CdS/TiNTA). XRD, UV Vis DRS, FTIR, FESEM, and EDX characterizations were carried out to evaluate crystallinity, band gap, morphology, and the presence of intended components.

The photocatalytic properties of CdS/TiNTA wereby means of the degradation of ciprofloxacin (CIP) as a type of antibiotics dominating the output of medical liquid waste in public waters[16]. CIP tends to accumulate in the aquatic environment due to its low biodegradability. This issue needs a concern to find intensive processing methods to reduce the harmful effects of this waste on the environment.

The study was intended to observe the ability of CdS/TiNTA photocatalysts to degrade CIP. The measurements of the hydrogen produced during the process were also carried out, considering that the photocatalyst can make water splitting reaction. At the same time, the waste sample used was dominated by water as the solvent. Thus, this study is expected to contribute to solve environmental problems while concurrently generating renewable energy carrier.

2. Materials and Methods

2.1. Materials

The materials used in this study included titanium plates (Shaanxi Yunzhong Metal Technology Co., LTD) each of which was in the size of 4 x 8 x 0.1 cm on which nanotubular structure of TiO_2 was grown. The chemicals used were $(CH_3COO)_2Cd$ (Merck), Na_2S (Merck), HF (Merck, 40%), HNO_3 (Merck, 65%), glycerol, NH_4F (Merck, 99.9%), NaOH 0.1 N (SmartLab), and Ciprofloxacin tablets of 500 mg. Meanwhile, the ultrasonic waves were generated by the Elmasonic type E30H, with a frequency of 50/60 Hz.

2.2. Preparation and synthesis

Titania plates were polished with sandpaper and washed with a chemical solution of HF-HNO_3-distilled water at a volume ratio of 1:3:46. The anodization process was carried out in a glycerol solution containing 0.5% wt HF and 25% v/v distilled water, followed by the immersion of Titania plates and stainless steel as the anode and cathode, respectively. This process was carried out using a direct current of 50 V for 2 hours [9].

The CdS/TiNTA nanocomposites were synthesized using the Successive Ionic Layer Adsorption and Reaction (SILAR) method. $(CH_3COO)_2Cd$ and Na_2S were used as the precursors at various concentrations of 0.05 M, 0.1 M, and 0.2 M, which were then abbreviated into CdS/TiNTA-S 0.05, CdS/TiNTA-S 0.1, and CdS/TiNTA-S 0.2, respectively.

The TiNTAs plates were firstly immersed in $(CH_3COO)_2Cd$ for a certain period, and then rinsed with distilled water, drained, and again dipped in Na_2S solution in one cycle. During this study, the cycles was taken six times, and the immersion time was in 5 minutes, based upon the optimal results obtained in previous study [8]. The variable observed in this synthesis process was the treatment during the SILAR. Furthermore, some plates were sonicated for 60 minutes, while other were synthesized without sonication. This treatment was also carried out on TiNTA plates that did not contain CdS to clarify its effect on TiNTA performance. The plates were further calcined in the furnace at 500^{o}C for 3 hours.

2.3. Photocatalyst characterization

The successful formation of photocatalyst material crystals and their size were analyzed using the XRD (Empyrean Series 3 Panalytical) test at 40 kV voltage and 30 mA current with Cu as its anode (Kα= 0.15406 nm). The morphology of the prepared sample (TiNTA and CdS/TiNTA) was observed using a Field Emission Scanning Electron Microscope (FESEM, FEI Inspect F50, and JEOL JIB-4610F). The UV-Vis test was used to observe the effect of adding CdS to the TiNTA surface on the energy bandgap value (Harrick Scientific Agilent Cary 600 UV-Vis DRS). The presence of the components or functional group on the plate surface was observed using the FTIR test (FTIR Nicolet iS5 Thermo scientific).

2.4. Evaluation of photocatalyst performance

The performance of the photocatalyst in degrading ciprofloxacin (CIP) solution and producing hydrogen gas was observed. In the photocatalytic process, plates with CdS/TiNTA nanocomposites on both sides of the surface are used. The CIP solution with a concentration of 10 ppm and a

volume of 500 ml was put into a quartz glass vessel, and the nanocomposite plate was mounted vertically. Here, the vessel was tightly closed to prevent the resulting gas from escaping from the system. Two mercury lamps @ 250 watts illuminated both sides of the plate, each consisting of 17.25% UV light and 82.75% Vis light, equivalent to a photon energy value of 2.75 eV. Observations were made every hour by measuring any changes in CIP concentration and the amount of hydrogen produced.

CIP concentration measurements were carried out using a UV-Vis spectrophotometer (Shimadzu, UVMini 1240), which worked on wavelengths 336nm. Equation (1) was used to calculate the decrease in CIP concentration.

$$CIP\ concentration\ ratio = C/C_0 \quad (1)$$

C_0 and C refer to the concentration of CIP in mg/L (ppm) at initial and at a certain time, respectively. The concentration of hydrogen produced by photocatalysis was analyzed every hour using a Gas Chromatography (Shimadzu GC-8A) system equipped with a Molecular Sieve (MS) Hydrogen 5 A column, with a known retention time for argon as the carrier gas.

3. Results and Discussion

3.1. Characterization of TiNTA and CdS/TiNTA nanocomposites

The photocatalyst synthesis resulted in TiNTAs plates and CdS/TiNTA nanocomposites were tested by XRD characterization to determine the crystals formation.

Table 1. Percentage of Anatase Content

Photocatalyst	Anatase, %
TiNTA without sonication	48.7
TiNTA with sonication	61.9
CdS/TiNTA without sonication	41.8
CdS/TiNTA with sonication	51.5

This test was carried out on four types of plates, consisting of two TiNTA plates which were synthesized with and without sonication. While other two plates were CdS/TiNTA nanocomposite plates abbreviated as CdS/TiNTA-nS and CdS/TiNTA-S, respectively describing nanocomposites synthesized with and without sonication. Figure 3 shows the peaks at 25.4º, 48º, and 54º, indicating the presence of anatase crystals and a small amount of rutile phase at an angle of 35º according to JCPDS No. 21-1272[17]. The high peaks at values of 2Θ at points 38º and 40.3º indicated the presence of Titania, which was used by Titania plates as a base material in the TiNTA synthesis. Meanwhile, hexagonal CdS crystals can be seen at the peaks located at 2Θ values around 24.8º, 43.7º, 47.8º and 51.8º, according to JCPDS No. 41-1049 [13].

The XRD analysis results also showed a number of differences in the anatase content of the different synthesized plates. TiNTA which was prepared by including sonication treatment in the synthesis process produced more anatase phase (61.9%) compared to the one by not including (48.7%). It experienced an increase in anatase content, which received sonication treatment, thereby indicating its contribution to the formation of anatase crystals during the synthesis process. The cavitation phenomenon, widely claimed to occur in the sonication process created the conditions of high temperature and pressure in a short time [18], and helpeds anatase crystals to form more intensively. The comparison between CdS/TiNTA nanocomposites synthesized by sonication showed similar conditions. The sonication treatment in the SILAR process produced a higher percentage of nanocomposites (51.5%) compared to those without sonication (41.8%). The decrease in the content of anatase crystals in the CdS/TiNTA nanocomposite when compared to TiNTA indicateeds the success of CdS entering the Titania nanotubes phase form nanocomposites. This then led to the prevention of anatase crystals from being monitored. CdS easily entereds the TiO_2 in its amorphous phase because its surface was more porous than the crystalline. The synthesis development process occurreds at this stage, which was different from previous study, where the process of attaching CdS was conducted after the calcination process of TiO_2 [15, 19-21]. Furthermore, its attachment to the TiO_2 crystal phase, after calcination, was very ineffective because the condition of the crystal surface was not too porous, thereby reducing the possibility of good contact between both substances.

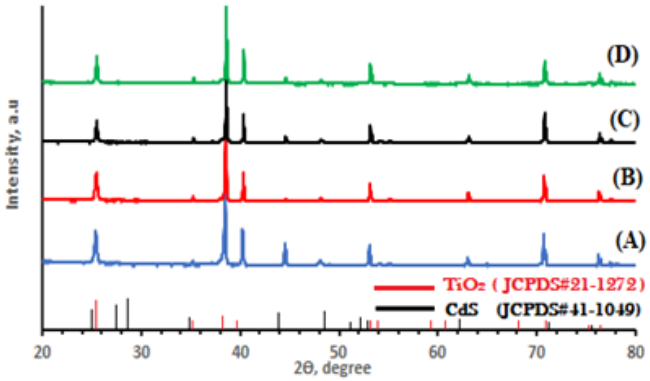

Fig. 1. XRD pattern of (A) TiNTA without sonication, (B) TiNTA with sonication, (C) CdS/TiNTA-nS, and (D) CdS/TiNTA-S

The results of the FESEM characterization showed that the synthesis method that has been carried out produces TiO_2 which hads a nanotube array morphology, with a relatively uniform inner diameter around 280 nm, and a wall thickness of 33 nm, as shown in Figure 2.

Figure 2 also compares the nanocomposite results obtained with and without sonication. Figure 2B shows the deposit of CdS on the surface of TiNTAs in the form of lumps that were not very evenly distributed. In contrast to the one obtained in the synthesis method with sonication treatment, as shown in Figure 2C, where the CdS deposits looked more uniform with a finer texture, so that at the right amount, the presence of CdS on the TiNTAs surface did not interfere with light penetration to the surface or the inside of TiNTAs tubes. The EDS analysis showed that the CdS/TiNTA nanocomposites synthesized by sonication treatment produced more CdS deposits than those not treated with sonication.

In the FT-IR spectrum, as shown in Figure 3, on CdS/TiNTA-S and CdS/TiNTA-nS, peaks appeared relatively in the same position. The peaks that appeared indicated the

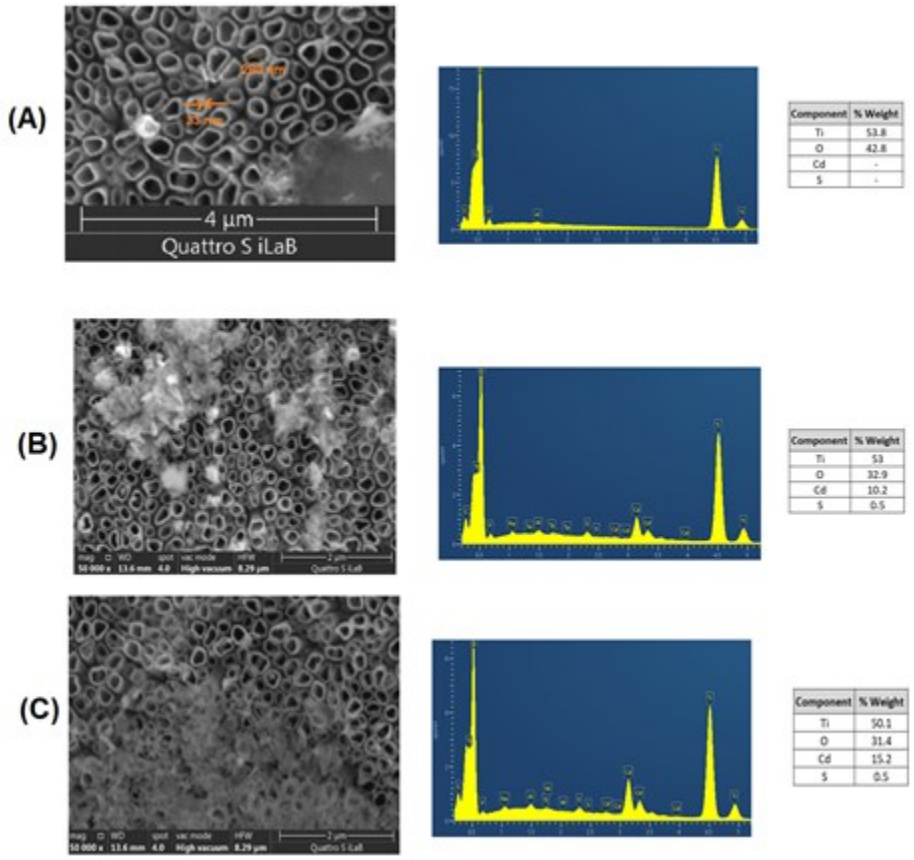

Fig. 2. FESEM image (left) and EDS (right) at various photocatalyst : (A) TiNTA, (B) CdS/TiNTA-nS, and (C) CdS/TiNTA-S

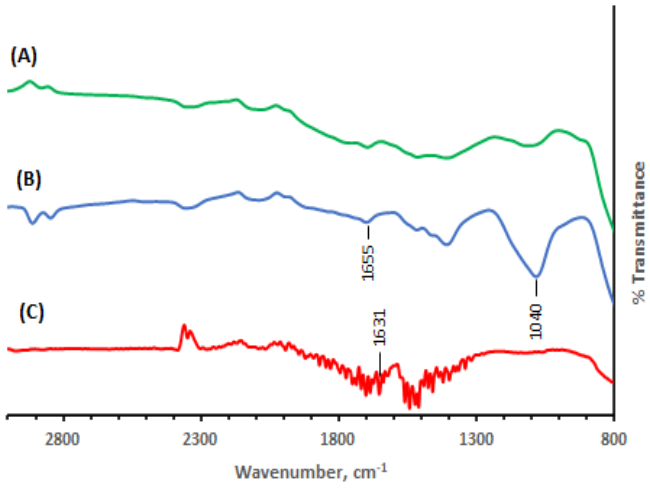

Fig. 3. The FT-IR spectrum of (A) CdS/TiNTA-S, (B) CdS/TiNTA-nS, and (C) TiNTA

presence of TiOH (1639 cm^{-1}), CdS (1040 cm^{-1}; 1655 cm^{-1}) and C=O (1650 cm^{-1}) [21,22]. The appearance of peaks at same position on the CdS/TiNTA-S plate compared to testing on the CdS/TiNTA-nS plate indicateds the possibility that CdS was present on the surface of the nanocomposite. On TiNTA plate that was characterized, the presence of TiOH(1639 cm^{-1}) and TiO_2 (1695 cm^{-1}) groups was seen in significant amounts DRS UV-Vis spectra of nanocomposites were then collected to assess the optical properties of samples. It can be seen in Figure 4(A) that there was a shift in absorbance on each plate, which indicateds the effect of the presence of nanocomposites and the sonication treatment during synthesis on the ability of the photocatalyst to absorb energy from exposure to ultraviolet and visible light.

When compared with various synthesis results, the CdS/TiNTA nanocomposites synthesized by sonication ztreatment (CdS/TiNTA-S) appeared to have the strongest absorption in the range of visible light and ultraviolet light. Even in the ultraviolet wavelength range (λ <380 nm), CdS/TiNTA-S hads better absorbance ability than TiNTA and CdS/TiNTA-nS.

This proveds that the synthesized nanocomposite, with sonication treatment, could produces a photocatalyst that could absorb light with a broader spectrum, covering the range of visible and ultraviolet light.

The measurement of the energy band gap by Kubelka Munk plot can be obtained from the intercept of the tangent line of $(F(R) = (\alpha h\upsilon)^{1/2})$ vs. energy curve at the horizontal axis, where h is Planck's constant, and υ refers to the frequency of the light. Figure 4(B) shows that CdS/TiNTA-S had the smallest value (Eg = 2.69 eV), thus enabling this nanocomposite to have a better ability to be activated by visible light and ultra violet light compared to other photocatalysts such as CdS/TiNTA-nS and TiNTA. This clearly illustrateds that the nanocomposite synthesis process carried out in the amorphous phase accompanied by sonication treatment could efficiently increase the contact

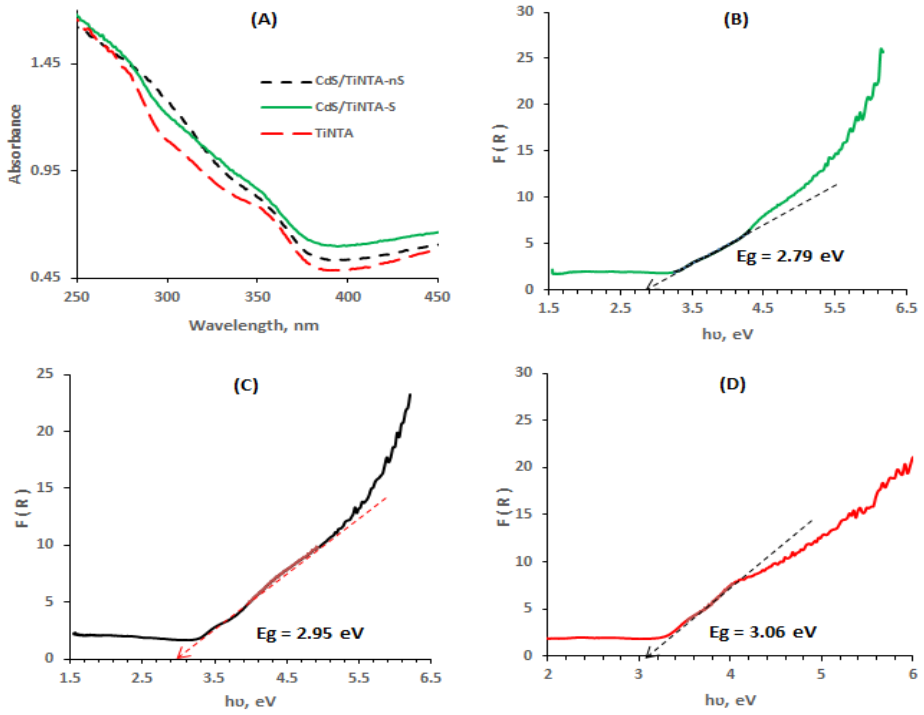

Fig. 4. (A) UV-Vis Absorption Spectra of various photocatalyst, and Kubelka Munk method for measurement energy bandgap of : (B) CdS/TiNTA-S, (C) CdS/TiNTA-nS, and (D) TiNTA

between CdS and TiNTA, resulting in a material that had good light absorbing ability in a broader light spectrum interval. This fact was also associated with higher crystallinity and aggregation of CdS nanoparticles, as confirmed by XRD and FESEM observations.

3.1. Photocatalyst performance

The performance of the synthesized TiNTA photocatalyst by sonication treatment has been tested and compared with the non-sonicated type. The mechanism of CIP degradation that may occur in the photocatalytic process using CdS/TiNTAs nanocomposites based on previous studies can be described as follows [23]:

$$CdS + h\upsilon \longrightarrow CdS\ (h_{VB}^{+} + e_{CB}^{-}) \quad (2)$$

$$TiO_2 + h\upsilon \longrightarrow TiO_2\ (h_{VB}^{+} + e_{CB}^{-}) \quad (3)$$

$$CdS\ (h_{VB}^{+} + e_{CB}^{-}) + TiO_2 \longrightarrow CdS(h_{VB}^{+}) + TiO_2(e_{CB}^{-}) \quad (4)$$

$$CdS(h_{VB}+) + OH^{-} \longrightarrow CdS + OH^{\bullet} \quad (5)$$

$$TiO_2(e_{CB}^{-}) + O_2 \longrightarrow TiO_2 + O_2^{\bullet-} \quad (6)$$

$$O_2^{\bullet-} + e_{CB}^{-} + 2H^{+} \longrightarrow H_2O_2 \quad (7)$$

$$O_2 + 2e_{CB}- \longrightarrow H_2O_2 \quad (8)$$

$$H_2O_2 + e_{CB}^{-} \longrightarrow OH^{\bullet} + OH^{-} \quad (9)$$

$$O_2^{\bullet-}, H_2O_2, OH^{\bullet}, h_{VB}^{+}, \ldots + \text{Ciprofloxacin} \longrightarrow \text{Degraded Products} \quad (10)$$

As a type of antibiotic that is difficult to degrade, the degradation reaction of CIP into simple compounds is a very long reaction and produces many intermediates [24,25]. Meanwhile, the production of hydrogen is possible because of the water splitting reaction as presented below.

$$TiO_2\ (e_{CB}^{-}) + 2H^{+} \longrightarrow TiO_2 + H_2 \quad (11)$$

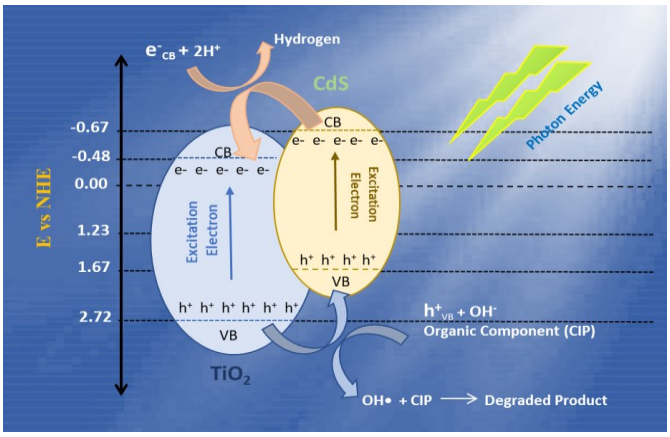

Fig. 5. The photocatalytic mechanisme of CdS/TiNTA heterojunction

The valence band positions for CdS and TiO_2 were 1.67 and 2.72 eV, respectively. Meanwhile, the position of the conduction band could be determined by adding the values of the valence band energy levels to the CdS and TiO_2 energy band gaps, i.e. 2.3 eV and 3.2 eV, respectively. Thermodynamically, these energy level differences allow for the transfer of electrons from the CdS conduction band to the TiO_2 conduction band and the transfer of holes from the TiO_2 valence band to the CdS valence band, as shown in Figure 5.

The process of transferring electrons and holes extends their transfer routes, thereby reducing the possibility of electron-hole recombination. As is well known, one of the obstacles encountered in using TiO_2 as a photocatalyst is its high recombination rate. The use of CdS and TiO_2 as a nanocomposite is expected to overcome this obstacle, while with a smaller CdS energy bandgap, it is believed that it also can expand the spectrum of light to be absorbed. Thus, the CdS/TiNTA nanocomposite is expected to be active in the UV light range and the visible light spectrum.

According to the photocatalytic reaction mechanism, oxidation reactions occur due to holes in the valence band, while reduction reactions occur due to electrons in the conduction band. Thus, in the CdS/TiNTA nanocomposite, there is a heterojunction scheme, as shown in Figure 5 and Equation (2) – (10), based on the position of electrons in the TiO_2 conduction band and holes in the CdS valence band, namely at -0.48 eV and 1.67 respectively. From the difference with the reduction energy level (H^+ /H_2 = 0.00 eV) and oxidation reactions ($H_2O/OH^{\bullet}$ = 1.23 eV), it can be analyzed that CdS/TiNTA will occur more easily in reduction reactions than oxidation reactions. This is because the difference in the conduction band with the reduction energy level is more significant, so thermodynamically, it will be easier for the reduction reaction to occur in the CdS/TiNTA nanocomposite.

In a study on photocatalyst performance, the performance of TiNTA photocatalyst was initially observed. An attempt was made to observe the effect of sonication during the synthesis of TiNTA on its performance in the photocatalytic process.

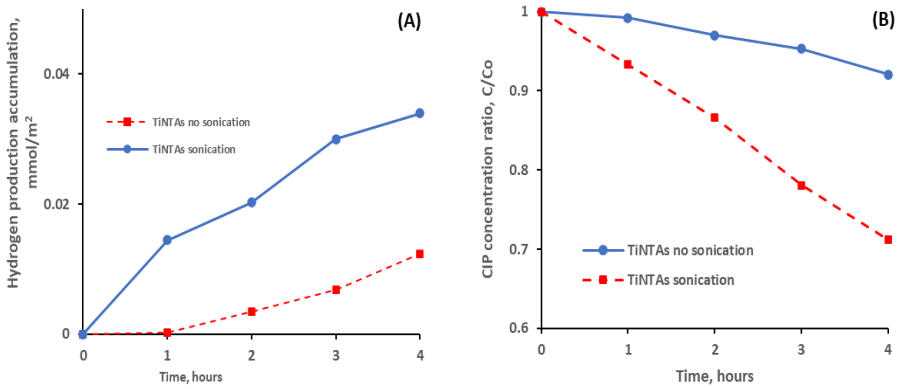

Fig. 6. The performance of sonicated and non-sonicated TiNTA in (A) producing hydrogen gas and (B) degrading CIP

As shown in Figure 6, the sonicated TiNTA was found much better at degrading CIP and producing hydrogen gas. This is in line with the XRD results in Figure 3, where an increasing anatase composition of sonicated TiNTA has allowed better performance in the photocatalytic process. However, based on the results of the UV-Vis DRS test, the two types of photocatalyst had relatively similar energy bandgap, and the presence of more anatase crystals significantly affected its performance.

The CdS/TiNTA nanocomposites synthesized using the SILAR method and sonication treatment were tested to determine their ability in photocatalysis. Several precursor concentration values of 0.05 M, 0.1 M, and 0.2 M were tried to obtain optimal performance. The concentration of 0.1 M provided superior performance in its ability to produce hydrogen gas and degrading CIP solutions, as shown in Figure 7. The presence of CdS and TiNTA as nanocomposites on the photocatalyst plate has provideds good synergy with the formation of a heterojunction mechanism analyzed to reduce the recombination rate and widen the range of photon energy that can activate the photocatalyst.

The use of precursor concentrations lower than the optimal value was inadequate to attach CdS to TiNTA as it preventeds the resulting nanocomposites from working well in the photocatalyst process. Conversely, a precursor concentration higher than 0.1 M provideds a shading effect on the photocatalyst surface due to excess CdS. This condition reduceds the photocatalyst's ability to degrade CIP and produce hydrogen gas.

The performance of the CdS/TiNTA nanocomposites synthesized by the SILAR method without sonication treatment was also tested in the photocatalyzed process of a

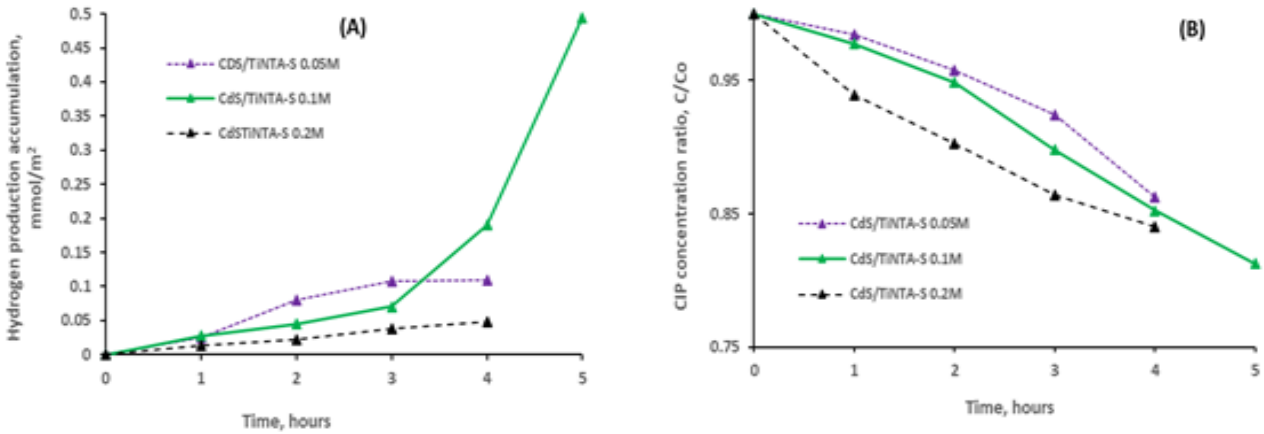

Fig. 7. Performance of CdS/TiNTA nanocomposites by sonication in (A) producing hydrogen gas and (B) degrading CIP

10 ppm CIP sample solution. Similar to the previous nanocomposites tests, observations were made with several variations in the precursor solution to obtain the concentration with optimal performance. Figure 8 shows that the precursor solution with a concentration of 0.1 M hads a significant ability to produce hydrogen gas while simultaneously degrading the CIP solution.

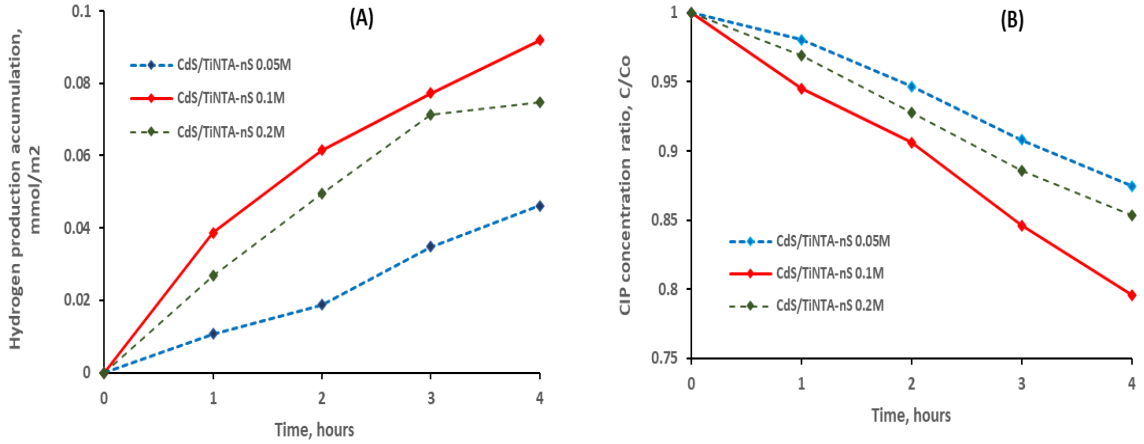

Fig. 8. Performance of CdS/TiNTA nanocomposites without sonication in (A) producing hydrogen gas and (B) degrading CIP

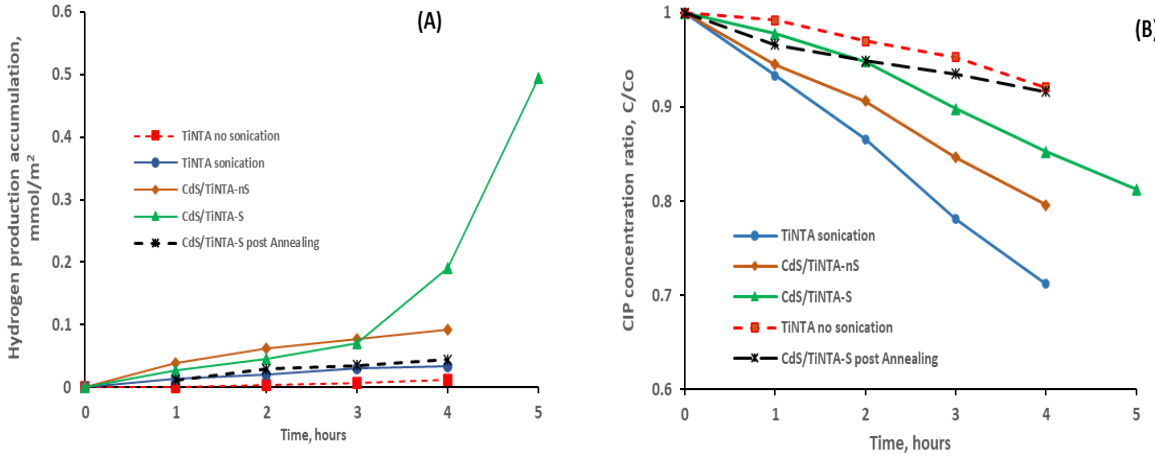

Figure 9. Summary of the performance of various photocatalysts in (A) producing hydrogen gas and (B) degrading CIP

To further clarify the effect of different treatments on photocatalyst performance, a comparison of photocatalyst performance from several synthesis processes was carried out, as shown in Figure 9. The figure also shows the performance of the synthesized CdS/TiNTA nanocomposites in previous studies, where the SILAR process was carried out in the TiO_2 crystal phase, and no sonication was applied during the synthesis [13-15, 26]. The results of the synthesis described by the abbreviation CdS/TiNTA-nS post Annealing showed performance that was not as good as the CdS/TiNTA-S nanocomposites, not even as good as CdS/TiNTA-nS. This fact proved that the CdS deposit process carried out in the amorphous phase of TiO_2 significantly affecteds the character of the resulting nanocomposite. It is suspected that the amount of CdS deposited has affecteds the nanocomposite's ability to degrade CIP and produce hydrogen.

It also can be seen that the CdS/TiNTA nanocomposites with sonication showed excellent performance in producing hydrogen gas. However, its ability to degrade CIP was still good compared to sonicated TiNTA. This is by considering that CdS is a semiconductor with a very good conduction band position in reduction reactions, but its valence band position is not very good in oxidation reactions. As the result, the coupling of CdS with TiNTA does not significantly affect the ability of the resulting nanocomposite to oxidize CIP.

CdS/TiNTA nanocomposite is a more advantageous photocatalyst for reducing H^+ ions into hydrogen gas. Based on the studies that have been carried out, the hydrogen recovery using CdS/TiNTA nanocomposites without sonication treatment was found at 0.092 mmol/m^2, which is twice the value of hydrogen recovery using TiNTA. Then the gain can be doubled again (0.19 mmol/m^2), using similar nanocomposites synthesized by sonication treatment and the SILAR synthesis method on the amorphous phase. However, the ability of CdS/TiNTA in terms of oxidizing CIP as a pollutant did not provide significant results which were believed in relation to the position of the CdS energy band which did not significantly affect the ability of the nanocomposite to oxidize CIP.

4. Conclusion

CdS/TiNTA synthesized by the SILAR method in the amorphous TiO_2 phase and subjected to sonication during the synthesis process provided the photocatalyst results with significantly increasing performance. The proposed method can enhance the material's crystallinity. CdS could be deposited well, producing nanocomposites with better light absorption capabilities and a smaller energy bandgap value, enabling photocatalysts to be active in a broader light spectrum. This conditions were confirmed by reading the characterization of XRD, FESEM, EDS, UV-Vis DRS, and FT-IR. Nanocomposite performance was tested in the photocatalytic process, and the improvement occurred mainly in terms of its ability to produce hydrogen gas. The photocatalyst synthesized by sonication during SILAR had twice better ability to produce hydrogen (0.191 mmol/m^2) compared to the photocatalyst synthesized without sonication (0.092 mmol/m^2). Compared to similar photocatalysts synthesized using the SILAR method in the crystalline phase, photocatalysts synthesized in the amorphous phase provided four times better ability to produce hydrogen (0.044 vs. 0.191 mmol/m^2). This highly sophisticated nanocomposite capability was related to the success of CdS adhering well to TiO_2 surface to form nanocomposites, so that the bandgap energy position of CdS that was strong in the reduction reaction greatly contributeds to improve the performance of the resulting photocatalyst in producing hydrogen gas through the water splitting.

Acknowledgements

The authors are grateful to Hibah Disertasi Doktor for the financial support from the Ministry of RistekDikti, Indonesia, with Contract Number: NKB-841/UN2.RST/HKP.05.00/2022. The authors are also grateful to the Department of Chemical Engineering, Faculty of Engineering, Universitas Indonesia, for the research facilities.

References

1. A. Fujishima, and K. Honda, *Electrochemical photolysis of water at a semiconductor electrode.* nature, 238 (1972) 37-38.
2. B. Liu, S. Su, W. Zhou, Y. Wang, D. Wei, L. Yao, et al., *Photo-reduction assisted synthesis of W-doped TiO 2 coupled with Au nanoparticles for highly efficient photocatalytic hydrogen evolution.* Cryst. Eng. Comm., 19 (2017) 675-683.
3. Z. Liu, J. Zhang, and W. Yan, *Enhanced photoelectrochemical water splitting of photoelectrode simultaneous decorated with cocatalysts based on spatial charge separation and transfer.* ACS Sustain. Chem. Eng., 6(2018) 3565-3574.
4. J.B. Priebe, J.R. Radnik, A.J. Lennox, M.-M. Pohl, M. Karnahl, D. Hollmann, et al., *Solar hydrogen production by plasmonic Au–TiO2 catalysts: impact of synthesis protocol and TiO2 phase on charge transfer efficiency and H2 evolution rates.* ACS Catal., 5 (2015) 2137-2148.
5. S.B. Patil, P.S. Basavarajappa, N. Ganganagappa, M. Jyothi, A. Raghu, and K.R. Reddy, *Recent advances in non-metals-doped TiO2 nanostructured photocatalysts for visible-light driven hydrogen production, CO2 reduction and air purification.* Int. J. Hydrog. Energy, 44 (2019) 13022-13039.
6. Y. Hou, , F. Zuo, A. Dagg, and P. Feng, *Visible light-driven α-Fe2O3 nanorod/graphene/BiV1–x Mo x O4 core/shell heterojunction array for efficient photoelectrochemical water splitting.* Nano lett., 12 (2012) 6464-6473.
7. J. S. Sagar, G.M.M., Jammula Koteswararao, Pradipkumar Dixit, *Studies on thermal and mechanical behavior of nano TiO2 -epoxy polymercomposite.* Commun. Sci. Technol., 7 (2022) 38-44.
8. A. Meng, B. Zhu, B. Zhong, L. Zhang, and B. Cheng, *Direct Z-scheme TiO2/CdS hierarchical photocatalyst for enhanced photocatalytic H2-production activity.* Appl. Surf. Sci., 422 (2017) 518-527.
9. M. Momeni and A. Mozafari, *The effect of number of SILAR cycles on morphological, optical and photo catalytic properties of cadmium sulfide–titania films.* J. Mater. Sci.: Mater. Electron., 27(2016) 10658-10666.
10. D. Esparza, G. Bustos-Ramirez, R. Carriles, T. López-Luke, I. Zarazúa, A. Martínez-Benítez, et al., *Studying the role of CdS on the TiO2 surface passivation to improve CdSeTe quantum dots sensitized solar cell.* J. Alloys Compd., 728 (2017) 1058-1064.
11. Y. Zhu, Y. Wang, Z. Chen, L. Qin, L. Yang, L. Zhu, et al., *Visible light induced photocatalysis on CdS quantum dots decorated TiO2 nanotube arrays.* Appl. Catal. A: Gen., 498 (2015) 159-166.
12. M. Qorbani, N. Naseri, O. Moradlou, R. Azimirad, and A. Moshfegh, *How CdS nanoparticles can influence TiO2 nanotube arrays in solar energy applications?* Appl. Catal. B: Environ., 162 (2015) 210-216.
13. C. Yu, Z. Zhang, Z. Dong, Y. Xiong, Y. Wang, Y. Liu, et al., *Fabrication of heterostructured CdS/TiO2 nanotube arrays composites for photoreduction of U (VI) under visible light.* J. Solid State Chem., 298 (2021) 122053.
14. A. Pieczyńska, P. Mazierski, W. Lisowski, T. Klimczuk, A. Zaleska-Medynska, and E. Siedlecka, *Effect of synthesis method parameters on properties and photoelectrocatalytic activity under solar irradiation of TiO2 nanotubes decorated with CdS quantum dots.* J. Environ. Chem. Eng., 9 (2021) 104816.
15. S. Wang, B. Zhu, M. Liu, L. Zhang, J. Yu, and M. Zhou, *Direct Z-scheme ZnO/CdS hierarchical photocatalyst for enhanced photocatalytic H2-production activity.* Appl. Catal. B: Environ., 243 (2019) 19-26.
16. I. Sanseverino, A. Navarro Cuenca, R. Loos, D. Marinov, and T. Lettieri, *State of the Art on the Contribution of Water to Antimicrobial Resistance.* Brussels: European Union (2018).
17. N.D. Johari, Z.M. Rosli, J.M. Juoi, and S.A. Yazid, *Comparison on the TiO2 crystalline phases deposited via dip and spin coating using green sol–gel route.* J. Mater. Res. Technol., 8(2019) 2350-2358.
18. J.C. Colmenares, E. Kuna, and P. Lisowski, *Synthesis of photoactive materials by sonication: Application in photocatalysis and solar cells.* Sonochemistry, (2017) 95-115.
19. X.-F. Gao, W.-T. Sun, Z.-D. Hu, G. Ai, Y.-L. Zhang, S. Feng, et al., *An efficient method to form heterojunction CdS/TiO2 photoelectrodes using highly ordered TiO2 nanotube array films.* J. Phys. Chem. A C, 113 (2009) 20481-20485.
20. Z. Zou, Y. Qiu, C. Xie, J. Xu, Y. Luo, C. Wang, et al., *CdS/TiO2 nanocomposite film and its enhanced photoelectric responses to dry air and formaldehyde induced by visible light at room temperature.* J. Alloys Compd., 645 (2015) 17-23.
21. J. Song, D. Zeng, Y. Xie, F. Zhang, S. Rao, F. Wang, et al., *Preparation of CdS nanoparticles-TiO2 nanorod hererojunction and their high-performance photocatalytic activity.* Catalysts, 10 (2020) 441.
22. B.S. Rao, B.R. Kumar, V.R. Reddy, T.S. Rao, and G. Chalapathi, *Preparation and characterization of CdS nanoparticles by chemical co-precipitation technique.* Chalcogenide Lett, 8 (2011) 177-185.
23. P. Wang, S. Xu, J. Wang, and X. Liu, *Photodeposition synthesis of CdS QDs-decorated TiO 2 for efficient photocatalytic degradation of metronidazole under visible light.* J. Mater. Sci.: Mater. Electron., 31(2020) 19797-19808.
24. H.-G. Guo, N.-Y. Gao, W.-H. Chu, L. Li, Y.-J. Zhang, J.-S. Gu, et al., *Photochemical degradation of ciprofloxacin in UV and UV/H 2 O 2 process: kinetics, parameters, and products.* Environ. Sci. Pollut. Res., 20 (2013) 3202-3213.
25. C. Aggelopoulos, M. Hatzisymeon, D. Tataraki, and G. Rassias, *Remediation of ciprofloxacin-contaminated soil by nanosecond pulsed*

dielectric barrier discharge plasma: Influencing factors and degradation mechanisms. J. Chem. Eng., 393 (2020) 124768.
26. H. Ungan, and T. Tekin, *Effect of the sonication and coating time on the photocatalytic degradation of TiO2, TiO2-Ag, and TiO2-ZnO thin film photocatalysts.* Chem. Eng. Commun.,207 (2020) 896-903.